Modeling of locally self-similar processes using multifractional Brownian motion of Riemann-Liouville type

S. V. Muniandy* and S. C. Lim
School of Physics, Universiti Kebangsaan Malaysia, 43600 UKM Bangi, Selangor, Malaysia
(Received 5 October 2000; published 22 March 2001)

Fractional Brownian motion (FBM) is widely used in the modeling of phenomena with power spectral density of power-law type. However, FBM has its limitation since it can only describe phenomena with monofractal structure or a uniform degree of irregularity characterized by the constant Holder exponent. For more realistic modeling, it is necessary to take into consideration the local variation of irregularity, with the Holder exponent allowed to vary with time (or space). One way to achieve such a generalization is to extend the standard FBM to multifractional Brownian motion (MBM) indexed by a Holder exponent that is a function of time. This paper proposes an alternative generalization to MBM based on the FBM defined by the Riemann-Liouville type of fractional integral. The local properties of the Riemann-Liouville MBM (RLMBM) are studied and they are found to be similar to that of the standard MBM. A numerical scheme to simulate the locally self-similar sample paths of the RLMBM for various types of time-varying Holder exponents is given. The local scaling exponents are estimated based on the local growth of the variance and the wavelet scalogram methods. Finally, an example of the possible applications of RLMBM in the modeling of multifractal time series is illustrated.

DOI: 10.1103/PhysRevE.63.046104 PACS number(s): 02.50.Ey, 05.40.−a

I. INTRODUCTION

There exist many phenomena that have generalized power-law spectral densities of the form $1/f^{\alpha}, 1<\alpha<3$. Examples include fluctuations in physical systems such as the anomalous diffusion, fluctuations of stock markets, biological and medical time series, bit rate of transfers in the internet traffics, etc. [1,2]. Such a property is usually associated with the long-range dependence of the processes involved or to the fractal nature of the sample paths. For these reasons, fractional Brownian motion (FBM) indexed by a constant Holder exponent (or Hurst index), H, is popular in the modeling and simulation of such phenomena.

Two main properties of FBM that guarantee the generalized power-law spectrum over many decades of frequency are the global self-similarity and the stationarity of the increment processes. Despite the success of FBM in the modeling of fractal phenomena characterized by single fractal dimension, D (or a constant Holder exponent H), it has been found to be too restrictive for many real situations that exhibit local self-similarity on a finite interval, whereby the local Holder exponent is time (or space) -dependent. To suit such an application, multifractional Brownian motion with the time-varying Holder function, $H(t)$, on a real line has been suggested [3,4]. Nevertheless, two equivalent representations of MBMs are based on the standard FBM introduced in [5] and [6], respectively, which include the memory from the distant past. Since the increment processes of the standard MBM are no longer stationary [a property that gives the main advantage to the standard FBM over the Riemann-Liouville type of fractional Brownian motion (RLFBM)], it would be interesting to consider whether an alternative MBM based on the extension of RLFBM can be considered in the same way as the standard MBM as far as applications are concerned. In fact, it has been shown in [7] that the large-time asymptotic RLFBM is a locally self-similar process.

In this paper, we study the multifractional Brownian motion based on the generalization of RLFBM as an example of a locally self-similar process that begins at the origin with the time-varying Holder exponent. We show that the local properties of the increment processes behave similarly to the standard MBM on the positive half of the real line. A simple numerical scheme to simulate locally self-similar sample paths for various time-varying Holder exponents is given. The local scaling exponents are estimated based on the local growth of variance and the wavelet scalogram methods. Finally, we suggest an application of the RLMBM for the modeling of multifractal financial time series.

II. SOME PROPERTIES OF MULTIFRACTIONAL BROWNIAN MOTION

The standard definition of fractional Brownian motion, which is widely accepted, is the version introduced by Mandelbrot and van Ness [5]:

$$B_H(t)=\frac{1}{\Gamma(H+\frac{1}{2})}\left\{\int_{-\infty}^{0}[(t-s)^{H-1/2}-(-s)^{H-1/2}]dB(s)+\int_0^t(t-s)^{H-1/2}dB(s)\right\}, \quad (1)$$

where the Holder exponent is restricted in the interval $0<H<1$. The standard FBM given in Eq. (1) is self-similar and its increments are stationary. These are the two properties that allow one to associate a generalized power-law spectrum to the process over a wide range of frequencies. The covariance of FBM has the following simple form:

*Corresponding author.

$$E[B_H(t_1)B_H(t_2)] = \frac{\sigma_H^2}{2}(|t_1|^{2H} + |t_2|^{2H} - |t_1 - t_2|^{2H}), \quad (2)$$

where

$$\sigma_H^2 = \text{var}(B_H(1)) = \frac{\Gamma(1-2H)\cos(H\pi)}{H\pi}. \quad (3)$$

There also exists another equivalent definition (up to a multiplicative constant) of FBM in the form of a harmonizable representation,

$$B_H(t) = \frac{1}{2\pi}\int_{-\infty}^{+\infty} \frac{e^{it\lambda} - 1}{|\lambda|^{H+1/2}} dB(\lambda). \quad (4)$$

A direct generalization of FBM to MBM can be carried out by replacing the Holder exponent H by a time-varying function, $H(t)$, satisfying $H:[0,\infty) \to (0,1)$. Throughout this paper, we shall assume that the Holder exponent is a continuous and smooth deterministic function of time, implying that $H(t+\tau) \approx H(t)$ for $\tau \to 0$.

So far, there exist at least two versions of standard MBMs [3,4] as a result of such generalizations on the definition in Eqs. (1) and (4), respectively. A proof of equivalence (up to a multiplicative deterministic function of time) between the different representations of MBMs can be found in [8,9]. For the scope of this study, we shall refer only to the definition of MBM given in [3], namely

$$X(t) = \frac{1}{\Gamma(H(t)+\frac{1}{2})}\left\{ \int_{-\infty}^{0} [(t-s)^{H(t)-1/2} - (-s)^{H(t)-1/2}] \times dB(s) + \int_0^t (t-s)^{H(t)-1/2} dB(s) \right\}. \quad (5)$$

Since the stochastic process defined in Eq. (5) has lost the stationary property of the increments, its self-similarity behavior is only valid locally within the interval of stationarity and the self-similarity property has to be replaced by the locally asymptotic self-similarity to be defined below.

A MBM, $X(t)$, indexed by the Holder exponent $H(t) \in C^{\beta}(R,(0,1))$ for $t \in R$ and some $\beta > \sup(H(t))$ is said to be locally asymptotically self-similar (LASS) at point t_o if [4,8]

$$\lim_{\rho \to 0^+} \left(\frac{X(t_o + \rho u) - X(t_o)}{\rho^{H(t_o)}} \right)_{u \in R} \equiv [B_{H(t_o)}(u)]_{u \in R}, \quad (6)$$

where the equality is up to a multiplicative deterministic function of time and $B_{H(t_o)}$ is the FBM indexed by $H(t_o)$. With the assumption that $H(t)$ is a β-Holder function such that $0 < \inf(H(t)) \leqslant \sup(H(t)) < \min(1\,\beta)$, one may approximate $H(t+\rho u) \approx H(t)$ as $\rho \to 0$.

For simplicity, we shall consider the normalized MBM, $Y(t) = X(t)/\sqrt{\sigma_{H(t)}}$, where

$$\sigma_{H(t)} = \frac{\Gamma(2-2H(t))\cos[H(t)\pi]}{H(t)\pi[2H(t)-1]}. \quad (7)$$

Therefore, the local covariance of the standard MBM is given by

$$E[Y(t+\tau)Y(t)] = \frac{1}{2}(|t+\tau|^{2H(t)} + |t|^{2H(t)} - |\tau|^{2H(t)}), \quad \tau \to 0, \quad (8)$$

where one assumes $H(t)$ is sufficiently smooth such that $H(t+\tau) \approx H(t)$ as $\tau \to 0$. The variance of the increment process becomes

$$E[|Y(t+\tau) - Y(t)|^2] = |\tau|^{2H(t)}, \quad \tau \to 0, \quad (9)$$

which is applicable for all time t.

One may remark that the local stationary behavior given by Eq. (9) is applicable for t on the real line, and the standard MBM [3,4] can be used for the modeling of locally self-similar processes with memories from the distant past. On the other hand, for processes that begin at the origin and evolve with the time-varying Holder exponent defined on $t > 0$, the standard MBM may not be an appropriate model. In the next section, we shall introduce the one-sided MBM based on the generalization of the fractional Brownian motion of Riemann-Liouville type [9].

III. ONE-SIDED MBM BASED ON THE RIEMANN-LIOUVILLE FRACTIONAL INTEGRAL

The fractional Brownian motion based on the Riemann-Liouville fractional integral (RLFBM) is defined as [10]

$$B_H(t)_+ = \frac{1}{\Gamma(H+\frac{1}{2})}\int_0^t (t-s)^{H-1/2} dB(s), \quad t \geqslant 0, \quad (10)$$

which holds for $H > 0$; it can also be extended to the range $-1/2 < H \leqslant 0$ as a generalized stochastic process. Despite having a simple form as compared to the standard FBM, the increments of this process are not stationary. As a result, one cannot associate it with a generalized spectral density of power-law type. This is the main reason why the RLFBM is seldom used in modeling physical systems exhibiting power-law spectral densities.

Since the standard MBM also does not have the globally stationary increment process, it is interesting to study the properties that MBM derived from the RLFBM in order to see whether both types of MBM have similar local properties. We consider the RLMBM as the generalization of Eq. (10) defined as

$$X_+(t) = \frac{1}{\Gamma(H(t)+\frac{1}{2})}\int_0^t (t-s)^{H(t)-1/2} dB(s). \quad (11)$$

The covariance of this Gaussian process for $0 < t_1 < t_2$ is calculated to be

$$E[X_+(t_1)X_+(t_2)] = \frac{2t_1^{H(t_1)+1/2}t_2^{H(t_2)-1/2}}{[2H(t_1)+1]\Gamma(H(t_1)+\frac{1}{2})\Gamma(H(t_2)+\frac{1}{2})} \times {}_2F_1\left(\frac{1}{2}-H(t_2),1,H(t_1)+\frac{3}{2},\frac{t_1}{t_2}\right). \quad (12)$$

Note that the variance takes the form $\sim t^{2H(t)}$ and furthermore it can be shown that the increments of the RLMBM share many similar behaviors to that of the standard MBM [9]. One can show that for $\tau_1/t \ll 1$ and $\tau_2/t \ll 1$ such that $|\tau_1-\tau_2| \to 0$,

$$E[\{X_+(t+\tau_1)-X_+(t)\}\{X_+(t+\tau_2)-X(t)\}] \sim \frac{1}{2}(|\tau_1|^{2H(t)}+|\tau_2|^{2H(t)}-|\tau_1-\tau_2|^{2H(t)}). \quad (13)$$

For $\tau_1=\tau_2=\tau$,

$$E[|X_+(t+\tau)-X_+(t)|^2] \sim |\tau|^{2H(t)}, \quad \tau/t \ll 1. \quad (14)$$

Thus, we have heuristically arrived at the locally asymptotic self-similarity property of the RLMBM and the interval of LASS improves as one gets far from the origin. Such a condition may be useful for modeling fractal anomalous diffusion phenomena [11]. In order to explore possible applications of modeling one-sided locally self-similar phenomena, it is necessary to have an accurate and efficient generator for the RLMBM.

IV. ON THE SIMULATION OF RLMBM

In this section, we describe a direct scheme to generate a discrete sequence of N points RLMBM, $X_+(t_j)$, with time sequence $H(t_j)$ where $0 \leq j \leq N$ and $t=[0,1] \in R^+$. We consider sampling the points from a set of N-sample paths of RLFBM generated for the respective pointwise values of $H(t_j)$ evaluated at $t_j = j/(N-1)$. Since the RLFBM generator is the basis of our scheme, a brief recall of one of its possible numerical simulations [12] is described below.

Consider the approximation of Eq. (10) for discrete time $t_j = j\Delta t$, $j \in Z^+$ and time step $\Delta t = 1/(N-1)$ as follows:

$$B_H(t_j)_+ = \frac{1}{\Gamma(H+\frac{1}{2})} \sum_{i=1}^{j} \int_{(i-1)\Delta t}^{i\Delta t} (t_j-\tau)^{H-1/2} dB(\tau). \quad (15)$$

Note that $dB(\tau)$ is the increment of Brownian motion, thus one can approximate

$$dB(\tau) = \left(\frac{\xi_i}{\sqrt{\Delta t}}\right) d\tau, \quad (16)$$

where ξ_i is the discrete sequence of Gaussian white noise with zero mean and unit variance. Upon integration Eq. (15) gives

$$B_H(t_j)_+ = \sum_{i=1}^{j} \left(\frac{\xi_i}{\sqrt{\Delta t}}\right) w_{j-i+1} \Delta t, \quad (17)$$

where the weighting function

$$w_i = \frac{1}{\Gamma(H+\frac{1}{2})} \left[\frac{t_i^{H+1/2}-(t_i-\Delta t)^{H+1/2}}{(H+1/2)\Delta t}\right]. \quad (18)$$

We shall use an improved form of the weighting function as suggested in [12], namely

$$\hat{w}_i = \frac{1}{\Gamma(H+1/2)} \left[\frac{t_i^{2H}-(t_i-\Delta t)^{2H}}{2H\Delta t}\right]^{1/2}, \quad (19)$$

which gives a more accurate scaling of the variance, i.e., $\mathrm{var}[B_H(t_j)] \sim t_j^{2H}$. Equations (17) and (19) form the generator of the discrete points of RLMBM simulation through the sampling procedure

$$X_+(t_j) = B_{H(t_j)}(t_j)_+, \quad 0 \leq j \leq N. \quad (20)$$

Using the generator described above, we simulated the sample paths of RLMBM for the following time-varying Holder exponents:

$$H_1(t) = \begin{cases} 0.4 & \text{for } 0 \leq t \leq 0.4 \\ 0.65 & \text{for } 0.4 < t \leq 1, \end{cases} \quad (21)$$

$$H_2(t) = at+b, \quad (22)$$

$$H_3(t) = ae^{-bt^2}+c, \quad a,b,c \in R, \quad (23)$$

where a,b,c are chosen arbitrarily for the sake of illustration and the sample paths are shown in Figs. 1(a)–1(c), respectively. All the variables considered here are dimensionless. Meanwhile, for applications of RLMBM in the modeling of locally self-similar processes, one usually has to estimate the time-varying Holder exponent from a single time series of the event with finite length. It is therefore crucial to have an accurate estimator that shows optimal compromises between the low variance in the estimated values and less bias on the choice of the estimator's window function.

V. ESTIMATION OF TIME-VARYING HOLDER EXPONENTS

There are a number of well-known methods for an accurate estimation of the constant Holder exponent of a monofractal time series. Among these, the rescaled range or R/S method and the Fourier power spectrum method are the most widely used on practical time series [13] and are usually implemented without any *a priori* assumption on the scaling behaviors that may exist in the time series. Since these methods are based on a linear log-log plot that results in a single value for the scaling exponent, they are not appropriate for the estimation of locally time-varying Holder exponents.

In order to have an unbiased estimator with low variance,

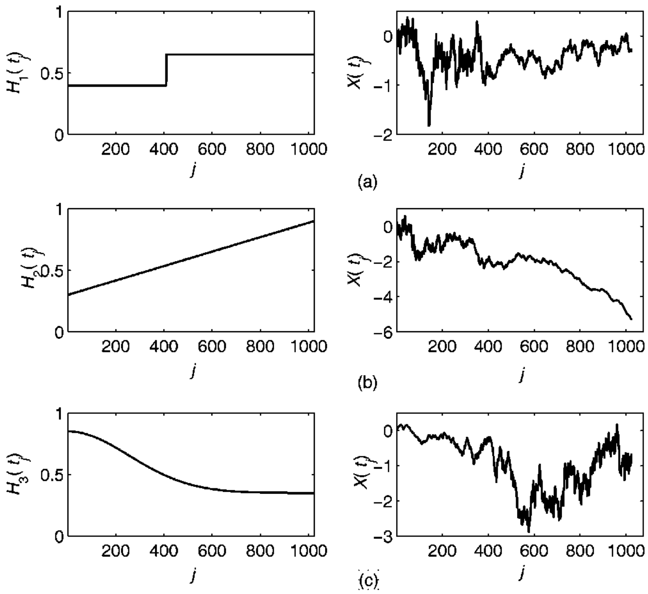

FIG. 1. The graphs of RLMBM with time-varying Holder exponent (a) $H_1(t)$, (b) $H_2(t)=0.6t+0.3$, and (c) $H_3(t)=0.5e^{-8t^2}+0.35$.

one has to consider an interval of local stationarity $|\tau|<\epsilon$, such that $H(t)$ is kept constant, i.e., $H(t)\approx H_t$ for $t\in[t-\epsilon/2,t+\epsilon/2]$. For an accurate estimation of $H(t)$ throughout the sample path, one needs to vary the interval ϵ with respect to the local regularity of $H(t)$. However, for simplicity, we have fixed the interval of stationary to be sufficiently small so as to provide a sufficient number of points k for a stable estimator. Based on the local growth of the increment processes, one may write a sequence [3]

$$S_k(j)=\frac{m}{N-1}\sum_{i=j-k/2}^{j+k/2}|X_{H_t}(i+1)-X_{H_t}(i)|,\quad 1<k<N, \tag{24}$$

where m is the largest integer not exceeding N/k. The local Holder exponent $H(t)$ at point $t=j/(N-1)$ is then given by

$$H_{j/(N-1)}=-\frac{\ln[\sqrt{\pi/2}S_k(j)]}{\ln(m-1)}. \tag{25}$$

The denominator in Eq. (25) has been modified to give a better estimate with respect to the small sample size with the length of the neighborhood, k. Here, we arbitrarily fix $k=8$ for all the computations bearing in mind that smaller values of k give better accuracies but larger fluctuations, and vice versa. The result of the estimation averaged over 10 sample paths for each function of $H(t)$ is given in Figs. 2(a)–2(c).

We may also consider the time-scale approach to the estimation of the local scaling exponent using the continuous wavelet transform defined as

$$T_X(t,a)=\frac{1}{\sqrt{|a|}}\int_{-\infty}^{+\infty}X(s)\psi^*\left(\frac{t-s}{a}\right)ds, \tag{26}$$

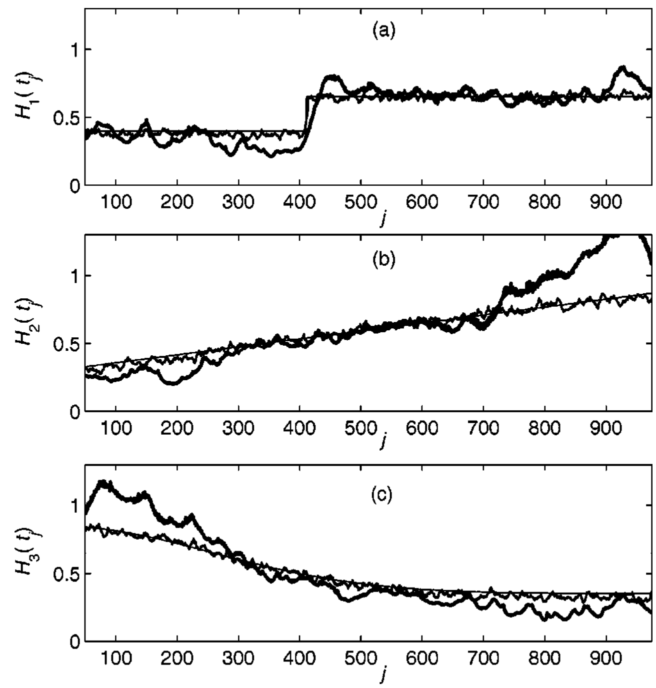

FIG. 2. The estimated time-varying Holder exponents for (a) $H_1(t)$, (b) $H_2(t)$, and (c) $H_3(t)$ compared to the respective input $H(t)$ functions (thin curves); intermediate curves, variance method; thick curves, scalogram method.

where $\psi(t)$ is an admissible wavelet with a large number of vanishing moments and a is the scaling parameter. In this paper, we shall use the Morlet wavelet. Since the RLMBM shows quite similar local properties to the standard MBM, many of the results obtained in [14,15] can be extended to the present situation. First, consider the local scaling of the increment processes of RLMBM at $t=t'$ as

$$E[|X(t'+\tau)-X(t')|^2]\sim|\tau|^{2H_t},$$

$$t'\in[t-\epsilon/2,t+\epsilon/2],\quad 0<|\tau|<\epsilon\ll 1. \tag{27}$$

Then by using the vanishing moment condition of the wavelets, we can write the wavelet coefficients as

$$T_X(t,a)=\frac{1}{\sqrt{|a|}}\int[X(t'+\tau)-X(t')]\psi^*\left(\frac{\tau-(t-t')}{a}\right)d\tau, \tag{28}$$

thereby giving the scalogram with the following scaling form:

$$\Omega_X(t,a)=E[|T_X(t,a)|^2]=a^{2H(t)+1}C\psi(t)\quad\text{and}$$

$$a\approx O(\tau)\to 0, \tag{29}$$

where $C_\psi(t)$ is a function that depends on the correlation of two wavelets with overlapping supports. It follows that the local Holder exponent is given by [15]

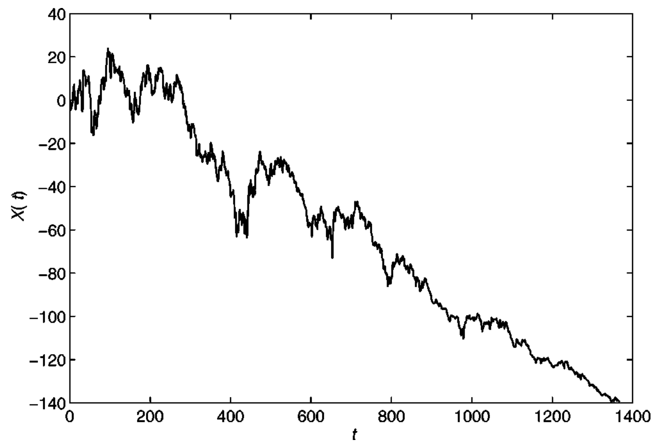

FIG. 3. The graph of the daily lowest of U.S. Dow Jones Industrial Average Stock Index.

$$H(t)=\frac{\frac{k}{2}\int a\Omega_X(t,a)e^{-ka}da}{\int \Omega_X(t,a)e^{-ka}da}-1, \quad (30)$$

with the smoothing function e^{-ka}, $k>0$. The value for k is chosen such that the local behavior (29) is feasible within the domain of the integration. For simplicity, we have arbitrarily fixed $k=8$, which in turn fixed the interval of local self-similarity in the same manner as the local growth of the increments method. One may remark that smaller values of k ensure that the support of the analyzing wavelet is well contained within the domain of the integration but produce large fluctuation in the estimation. Incorporating Eqs. (27) into Eq. (28) allows one to estimate the time-varying Holder exponent as given by Eq. (30) for the sample paths generated above and the results are compared to the variance-based method in Figs. 2(a)–2(c).

One may notice the poor performance of the wavelet scalogram method, which is mainly due to the finite resolution of the sample path, and furthermore we have fixed the number of octaves in the scalogram estimation throughout the graphs. A better estimate would be to consider an adaptive window with variable window sizes. We recall here the similar observation made in [3] that the variance method performs better compared to other schemes such as the spectral or the wavelet-based estimations. Therefore, we adopt the time-varying $H(t)$ estimator based on the variance method to suggest one possible application of RLMBM in the modeling of financial time series.

VI. MULTIFRACTIONAL MODELING OF FINANCIAL TIME SERIES

FBM has been useful as a model in accordance with the fractal market hypothesis to explain the scaling behaviors and the long-range dependences in financial time series [16]. One can associate the values $0<H<1/2$ to the antipersistent behaviors in the time series, where any positive increment in the past will be followed by a negative increment in the future and vice versa. Meanwhile, the range $1/2<H<1$ corresponds to persistent characteristics in the time series, i.e., any positive increment in the past will persist in the future and likewise for negative increments. Such a description has been found to be useful in the predictability and analysis of trends in financial and meteorological time series. On the other hand, the Holder exponent H can also be used to describe the fractal characteristic of the sample paths where the global fractal dimension D_H of the graph is given by $D_H=2-H$.

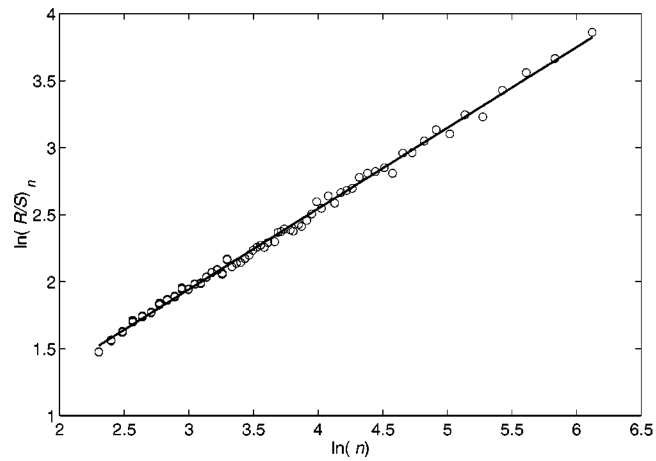

FIG. 4. Log-log plot of the R/S analysis of the financial time series.

In this paper, we examine the local scaling properties of the U.S. Dow Jones Industrial Average Stock Index for the duration of 3 January 1995 until 31 May 2000 and here we study the time series for the daily lowest index as shown in Fig. 3 (the graph has been shifted to begin at the origin and to be normalized). A practical monofractal method widely used in the estimation of the Holder exponent is the rescaled-range R/S method. The rescaled range is calculated by first rescaling the data, X_r, by subtracting the sample mean, $\hat{X}$,

$$Z_r=(X_r-\hat{X}), \quad r=1,\ldots,n, \quad (31)$$

where n is the number of points in the range. Denoting Y as the cumulative time series, the adjusted range is then defined as

$$R_n=\max\{Y_1,\ldots,Y_n\}-\min\{Y_1,\ldots,Y_n\}. \quad (32)$$

Upon dividing Eq. (32) by the standard deviation, $S_n=n^{-1/2}\sqrt{\overline{(X_r-\hat{X})^2}}$, one obtains the rescaled-range relationship

$$(R/S)_n=Cn^H, \quad (33)$$

where C is a constant. The slope of the log-log plot of Eq. (33) gives the empirical Holder exponent of the time series. The result of the R/S analysis on the Dow Jones time series is shown in Fig. 4, where the linear least-squares fitting gives $H=0.60\pm0.03$. The R/S method gives an average value for the Holder exponent of the time series and it has been useful for the fractal analysis of time series that exhibits monofractal behavior. In the case of financial time series shown in Fig.

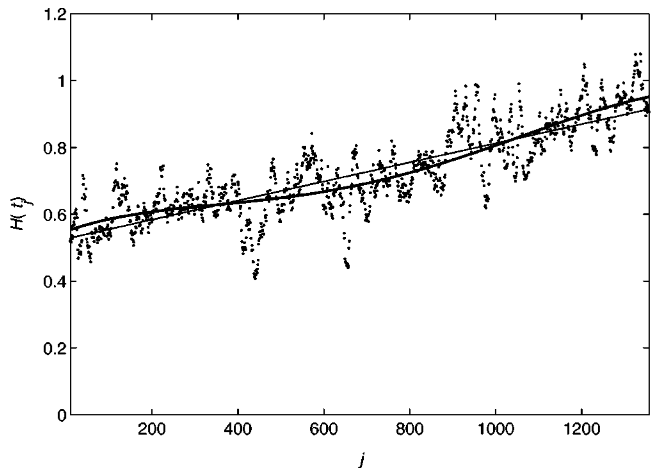

FIG. 5. The pointwise Holder exponent of the financial time series estimated using the variance method fitted with a linear $H(t)$ function (thin curve); thick curve, a fourth-order polynomial $H'(t)$.

3, it is obvious that the regularity of the sample path is not uniform throughout the graph and a monofractal description is rather inadequate.

Detailed analysis of financial time series has provided the evidence of multifractality [17,18] whereby there exists a finite set of Holder exponents in the time series. The usual notion of multifractality is based on the scaling behavior of structure functions:

$$S_p(\tau)=E\{[X(t+\tau)-X(t)]^p\}\sim\tau^{\xi_p}, \quad p\in Z^+, \tag{34}$$

where ξ_p is a nonlinear function [19,20]. We remark that by considering $S_2(t,\tau)=E[|X(t+\tau)-X(t)|^2]\sim\tau^{2H(t)}$, $\tau\to 0$, our approach provides an alternative description of time-dependent multifractal behavior for Gaussian time series characterized by the time-varying Holder exponent $H(t)$.

Based on the estimator given in Eqs. (24) and (25), we determine the empirical time-varying Holder exponents for the time series shown in Fig. 3. The results of least-squares fitting using a first-order polynomial, $H(t)=0.003t+0.527$ (χ^2 error$=7.67$), and a fourth-order polynomial, $H'(t)=(-4.572\times10^{-13})t^4+(1.301\times10^{-9})t^3-(1.037\times10^{-6})t^2+0.0005t+0.549$ (χ^2 error$=6.90$), are shown in Fig. 5. Even though the nonlinear fitting gives a better description of the local variation of Holder exponents, one has to allow for the inaccuracy of the estimator with a finite window length that causes the fluctuation in the estimation. For purposes of illustration, we may just consider the linear approximation for the increasing trend, and it is found that the daily lowest of the U.S. Dow Jones Industrial Average Stock Index exhibits local self-similarity with time-varying Holder exponents that fall approximately within 0.4 and 0.9. This observation conforms to the multifractal properties of financial time series by exhibiting that there exists a finite set of pointwise Holder singularity exponents. A monofractal estimation method such as the R/S analysis will only give the global average value of the Holder exponent based on the assumption that the time series has a uniform degree of irregularity, while the standard multifractal singularity spectrum describes the probablity distribution of the Holder exponents occurring in the time series. Both methods, however, do not give information on the time-dependent local self-similarity feature.

On the robustness of the estimation, one may remark that the large fluctuations in the pointwise values of $H(t)$ are mainly due to finite resolution of the estimator's window length used on a single time series of the event. However, the globally increasing trend in the estimated $H(t)$ for the time series depicted the time-varying multifractal behaviors, which can be modeled by locally self-similar processes such as the RLMBM introduced in this study.

VII. CONCLUSIONS

We have described the local self-similarity properties of RLMBM, which is shown to share many similar characteristics of the standard MBM especially in correspondence with the increments of the two processes. Since the stationarity of the increment processes is longer than the cornerstone of the standard MBM, one now has a choice of model for the study of locally self-similar processes based on the amount of memory to be integrated into the system. For processes that begin at the origin, we suggest that the RLMBM may be a suitable model compared to the standard MBM. We have also demonstrated a direct and simple scheme for the generator of RLMBM based on a method of sampling using a set of N-sample paths of RLFBM generated for the respective pointwise values of $H(t_j)$ evaluated at $t_j=j/(N-1)$. The time-varying Holder exponents estimated using the local variance method have been found to be more accurate compared to the scalogram method (see, for example, [3]) and this can also be related to the disadvantage of fixing the sampling window length in the latter [14] and on the sensitivity of the choice of mother wavelet. However, we believe that both methods should improve with adaptive sampling window length techniques.

Finally, we illustrated one possible application of RLMBM in the modeling of time-varying multifractality in financial time series. In contrast to the standard multifractal technique, which focuses on the probability distribution of the singularity spectrum, the method mentioned here gives an alternative description of the pointwise multifractal behavior of inhomogeneous time series or locally self-similar processes. It is found that to the first-order approximation, the daily lowest of the U.S. Dow Jones Industrial Average Stock Index exhibits local self-similarity with time-varying Holder exponents that increase from roughly $H\sim0.5$ to $H\sim0.9$ during the period of 3 January 1995 until 31 May 2000. A monofractal estimator such as the R/S analysis would only give the global average value of the Holder exponent ($H\simeq0.6$), thus implying a single trend of long-range dependence throughout the time series. Our results are also consistent with the multifractal properties of financial time series by showing that there exists a finite set of pointwise Holder singularity exponents. Other possible applications include the modeling of queing processes and ethernet traffic flows [21,22], which are currently under investigation.

ACKNOWLEDGMENTS

This research is supported by the Malaysian Ministry of Science, Technology and Environment under IPRA Grant No. 09-02-02-0092. S.C.L would like to thank Deutscher Akademischer Austauschdienst (DAAD) for financial support during his research visit to Institut fur Mathematik, Technische Universitat Clausthal, Germany, where parts of this work were carried out, and Michael Demuth for hospitality.

[1] B.B. Mandelbrot, *Multifractals and 1/f Noise: Wild Self-Affinity in Physics* (Springer Verlag, New York, 1999).
[2] H.E. Stanley, Rev. Mod. Phys. **71**, S358 (1999).
[3] R.F. Peltier and J. Levy-Vehel, INRIA Technical Report No. 2645 (1995) (unpublished).
[4] A. Benassi, S. Jaffard, and D. Roux, Revista Math. Iberoamericana **13**, 19 (1997).
[5] B.B. Mandelbrot and J.W. van Ness, SIAM Rev. **10**, 422 (1968).
[6] A.M. Yaglom, Am. Math. Soc. Trans. **8**, 37 (1955).
[7] S.C. Lim and V.M. Sithi, Phys. Lett. A **206**, 311 (1995).
[8] S. Cohen, in *Fractals: Theory and Applications in Engineering*, edited by M. Dekking *et al*. (Springer, Berlin, 1999), p. 3.
[9] S.C. Lim and S.V. Muniandy, Phys. Lett. A **266**, 140 (2000).
[10] J.A. Barnes and D.W. Allan, Proc. IEEE **54**, 176 (1966).
[11] T.F. Nonnenmacher and R. Metzler, Fractals **3**, 557 (1995).
[12] S. Rambaldi and O. Pinazza, Physica D **208**, 21 (1994).
[13] H.M. Hastings, and G. Sugihara, *Fractals: A User's Guide for the Natural Sciences* (Oxford Science, Oxford, 1993).
[14] P. Goncalves, and P. Abry (unpublished).
[15] P. Flandrin, *Time-Frequency/Time-Scale Analysis* (Academic Press, San Diego, 1999).
[16] E.E. Peters, *Fractal Market Analysis: Applying Chaos Theory to Investment and Economics* (John Wiley & Sons, New York, 1994).
[17] Y. Liu, P. Cizeau, M. Meyer, C.K. Peng, and H.E. Stanley, Physica A **245**, 437 (1997).
[18] A. Arneodo, J.F. Muzy, and D. Sornette, Eur. Phys. J. B **2**, 277 (1998).
[19] U. Frisch and G. Parisi, in *Turbulence and Predictability in Geophysical Fluid Dynamics and Climate Dynamics,* edited by M. Ghil *et al*. (North Holland, Amsterdam, 1985), p. 84.
[20] J.F. Muzy, E. Bacry, and A. Arneodo, Phys. Rev. Lett. **67**, 3515 (1991).
[21] M.S. Taqqu, V. Teverovsky, and W. Willinger, Fractals **5**, 63 (1997).
[22] W. Willinger, M.S. Taqqu, R. Sherman, and D.V. Wilson, IEEE Trans. Networking **5**, 71 (1997).